Fizika Nizkikh Temperatur, 2006, v. 32, No. 11, p. 1320–1329

Nonlinear and shock waves in superfluid He II

G.V. Kolmakov[1,2], V.B. Efimov[1,2], A. N. Ganshin[2], P.V.E. McClintock[2], E.V. Lebedeva[1], and L.P. Mezhov-Deglin[1]

[1] *Institute of Solid State Physics RAS, Chernogolovka 142432, Russia*
E-mail: mezhov@issp.ac.ru

[2] *Lancaster University, Lancaster, LA1 4YB, UK*
E-mail: g.kolmakov@lancaster.ac.uk

Received May 31, 2006

We review studies of the generation and propagation of nonlinear and shock sound waves in He II (the superfluid phase of ^{4}He), both under the saturated vapor pressure (SVP) and at elevated pressures. The evolution in shape of second and first sound waves excited by a pulsed heater has been investigated for increasing power W of the heat pulse. It has been found that, by increasing the pressure P from SVP up to 25 atm, the temperature T_α, at which the nonlinearity coefficient α of second sound reverse its sign, is decreased from 1.88 to 1.58 K. Thus at all pressures there exists a wide temperature range below T_λ where α is negative, so that the temperature discontinuity (shock front) should be formed at the center of a propagating bipolar pulse of second sound. Numerical estimates show that, with rising pressure, the amplitude ratio of linear first and second sound waves generated by the heater at small W should increase significantly. This effect has allowed us to observe at $P = 13.3$ atm a linear wave of heating (rarefaction) in first sound, and its transformation to a shock wave of cooling (compression). Measurements made at high W for pressures above and below the critical pressure in He II, $P_{cr} = 2.2$ atm, suggest that the main reason for initiation of the first sound compression wave is strong thermal expansion of a layer of He I (the normal phase) created at the heater-He II interface when W exceeds a critical value. Experiments with nonlinear second sound waves in a high-quality resonator show that, when the driving amplitude of the second sound is sufficiently high, multiple harmonics of second sound waves are generated over a wide range of frequencies due to nonlinearity. At sufficiently high frequencies the nonlinear transfer of the wave energy to sequentially higher wave numbers is terminated by the viscous damping of the waves.

PACS: 68.03.Kn, **47.35.+i**, 47.27.Gs

Keywords: first and second sound, nonlinearity, acoustic turbulence.

1. Introduction

First of all, we are much indebted to the Editorial Board of the *Low Temperature Physics* journal for their invitation to report the results of our recent studies in the special issue devoted to 100-th anniversary of the famous scientist A.F. Prikhot'ko.

We review here experimental and theoretical investigations of the peculiarities of nonlinear evolution of solitary second and first sound pulses propagating in superfluid ^{4}He, and of a second sound standing wave in a high-Q resonator filled with He II, the superfluid phase of ^{4}He. Entropy waves (second sound) are a macroscopic quantum effect that may be observed in superfluids and perfect crystals [1–3]. The properties of second sound in He II have been studied extensively, both experimentally and theoretically. More recently, attention has been focused on the nonlinear acoustic properties of He II [4–8].

It is known [1–3,9–11] that second sound is characterized by rather strong nonlinear properties. These lead to the formation of a shock wave (temperature discontinuity) during the propagation of a finite-amplitude wave in He II, at short distances from the source (heater). The velocity of a traveling second

sound wave depends on its amplitude and, to a first approximation, can be written:

$$u_2 = u_{20}(1 + \alpha\, \delta T_2), \qquad (1)$$

where δT_2 is the wave amplitude, u_{20} is the velocity of a wave of infinitely small amplitude, and α is the nonlinearity coefficient of second sound, which is determined by the relation [2]

$$\alpha = \frac{\partial}{\partial T} \ln \left(u_{20}^3 \frac{C}{T} \right), \qquad (2)$$

where C is the heat capacity per unit mass of liquid helium at constant pressure, and T is the temperature.

The nonlinearity coefficient α of second sound may be either positive and negative, depending on the temperature and pressure [2,10,12]. Under the saturated vapor pressure (SVP), in the region of roton second sound (i.e. at $T > 0.9$ K) the nonlinearity coefficient is positive ($\alpha > 0$) at temperatures $T < T_\alpha = 1.88$ K (like the nonlinearity coefficient of conventional sound waves in ordinary media), but it is negative in the range $T_\alpha < T < T_\lambda$. Here $T_\lambda = 2.176$ K is the temperature of the superfluid-to-normal (He II to He I) transition. At $T = T_\alpha$ the nonlinearity coefficient passes through zero.

If $T \neq T_\alpha$, the nonlinear evolution leads to the creation of a shock in the profile of a travelling second sound pulse. During the propagation of a plane, one-dimensional wave of heating (compression) of second sound ($\delta T_2 > 0$), the shock appears at the front of the propagating wave at temperatures 1 K $< T < T_\alpha$, and on the trailing edge of the wave for temperatures $T_\alpha < T < T_\lambda$ (see, for example, Fig. 1). The width of the shock front l_f is defined by both the nonlinearity coefficient α and the dissipation coefficient γ of second sound. In the hydrodynamic regime, where the shock front width exceeds greatly the mean free path of rotons, one has $l_f = \gamma/\alpha\delta T_2$ for the shock front width, and $v_f = u_{20} + \alpha\delta T_2/2$ for the velocity of shock propagation [1,2].

At large distances L from the heater the profile of a one-dimensional shock pulse eventually acquires a triangular form. The dependence of the length of the triangle (duration of the pulse τ) and its height (the temperature jump at the shock front δT_2) on the distance can be described by a universal power law

$$\tau = \text{const}\ (\alpha L)^{1/2}, \quad \delta T_2 = \text{const}\ (\alpha L)^{-1/2}, \qquad (3)$$

where the constants depend on the initial shape of the second sound pulse. It is important to note here that the evolution of a developed shock wave (i.e., the dependence of the parameters of the triangle on distance) is governed only by the value of the nonlinearity coefficient and does not depend on the value of the dissipation coefficient γ. The entropy production rate dS/dt at the shock front due to dissipative processes remains finite as the dissipation coefficient γ tends to zero, because the small value of γ is compensated by a large temperature gradient $dT/dx \sim \delta T_2/l_f$.

2. Propagation of nonlinear second sound pulses in He II

2.1. Evolution of the shape of second sound pulses with reduction of the temperature

The experimental arrangements were similar to those used in our earlier studies of nonlinear and shock second sound pulse propagation in He II [9,11]. Figure 1,*a* shows the evolution in shape of planar second sound pulses excited by a rectangular heat pulse at temperature $T = 2.10$ K under pressure $P = 3$ atm ($\alpha < 0$) [12]. The time duration of the electrical pulse applied to the resistive heater was $\tau_e = 10$ μs. The

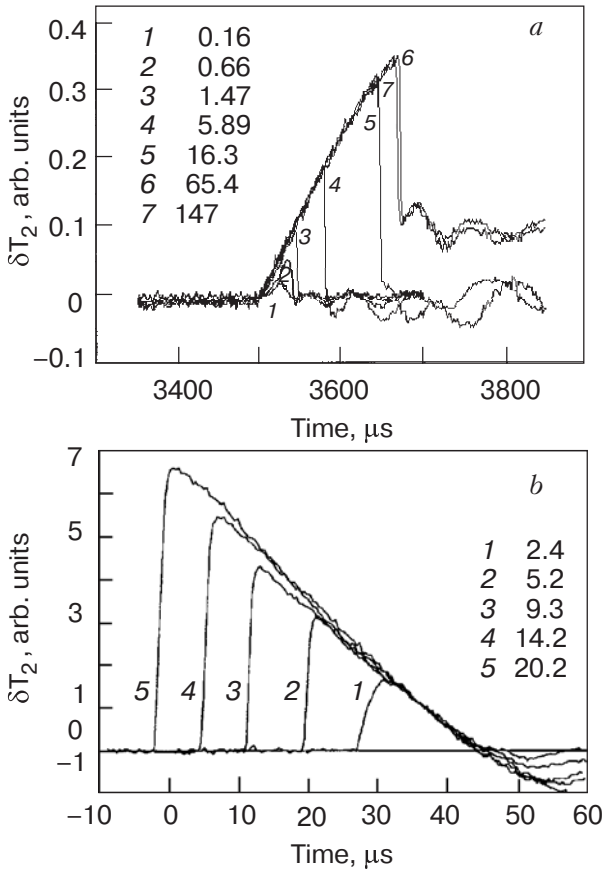

Fig. 1. Evolution in shape of planar second sound waves for increasing heat flux density W from the heater, where δT_2 is the temperature change measured at the bolometer: for a He II bath temperature of $T = 2.10$ K ($\alpha < 0$), pressure $P = 3$ atm (*a*); for $T = 1.50$ K ($\alpha > 0$), pressure $P = P_{SVP}$ (*b*). The numbers beside the curves indicate the heat flux density W expressed in W/cm^2. The time duration of the electrical pulse to the heater was $\tau_e = 10$ μs.

numbers beside the curves correspond to different heat flux densities W from the heater. The waves were detected by a superconducting film bolometer [13]. At small $W < 0.7$ W/cm^2 the bolometer detected linear waves (curves *1*, *2*) of amplitude δT_2 proportional to W. Above $W = 1$ W/cm^2 and up to 17 W/cm^2 the pulse shape is close to triangular (linear waves transform to planar shock waves, curves *3*–*5*). The amplitude of the triangular pulse δT_2 and its width increase in proportion to $W^{1/2}$. Above 30 W/cm^2 (curves *6* and *7*) the amplitude and the width of the pulse depend weakly on W (the range of saturation).

Figure 1,*b* shows the evolution of the profile of a second sound pulse at $T = 1.50$ K ($\alpha > 0$) under the SVP, $P = P_{SVP}$, while the heat flux density increases from $W = 2.4$ W/cm^2 to 20.2 W/cm^2, at a constant distance $L = 2.5$ cm from the heater [14]. The heater pulse duration was $\tau_e = 10$ μs. We see that the slope of profile $a = \delta T_2/\tau$ does not depend on W: in accordance with the general relations (3), the value $a = u_2/\alpha L$.

Creation of the shock on the trailing edge of a compression wave at $T > T_\alpha$ (or at the front of a rarefaction wave for $\delta T_2 < 0$) is a specific property of second sound in He II [2]. At temperatures very close to T_λ the nonlinearity coefficient tends to infinity according to the power law [7] $\alpha \sim \varepsilon^{-1}$, where $\varepsilon = (T_\lambda - T)/T_\lambda$ is the reduced temperature. Near the lambda transition the nonlinearity therefore plays a crucial role even for the smallest amplitudes δT_2.

We discuss here the evolution in the shape of short second sound pulses of the relatively small amplitude $|\delta T_2| < 10^{-2}$ K, so that we can neglect possible creation of quantum vortices at the shock front and the resultant wave-vortex interactions. For small amplitudes, the description of the nonlinear evolution of the second sound wave can be confined to the first terms in the expansion of the velocity u_2 in δT_2, as done in Eq. (1). Under this approximation the amplitude of a second sound pulse at small W (linear wave) should be proportional to W, i.e., $\delta T_2 \propto W \propto U^2$ (here U is a voltage applied to the heater). At higher W, where a shock wave is formed, the amplitude of the propagating triangular pulse should be proportional to $\delta T_2 \propto W^{1/2} \propto U$.

The experimental dependence of the amplitude of the pulse plotted as $\delta T_2(U)$ (left-side scale, open circles) and $\delta T_2^{1/2}(U)$ (right-side scale, solid circles) presented in Fig. 2 was reconstructed from the measurements shown in Fig. 1,*a* ($T = 2.10$ K, $P = 3$ atm, and heater pulse duration $\tau_e = 10$ μs).

At high W the amplitude of second sound pulses saturates, as can be seen from Figs. 1 and 2. A similar dependence was observed at $P = 3$ atm and $T = 1.7$ K, where the nonlinearity coefficient $\alpha > 0$. All the

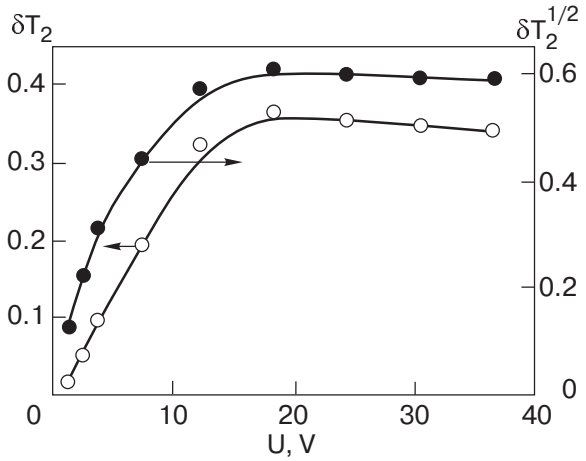

Fig. 2. Dependence of the amplitude of second sound wave δT_2 on the pulsed voltage U to the heater, reconstructed from Fig. 1,*a* (left-side scale, open circles), and the dependence on $\delta T_2^{1/2}$ on U (right-side scale, solid circles). Arrows show the proper scale of ordinates.

curves $\delta T_2(U)$ observed at different pressures and temperatures in our studies look much the same. Similar saturation effects at high W were reported in [15,16]. A detailed discussion of the reasons for the saturation lies beyond the scope of the present paper, but one reason could be the attenuation of the propagating second sound wave by vortices in the bulk of the He II [17]. However it follows from our observations (see Sec. 2.4) that, along with the nonlinear second sound wave, a heater should generate also a first sound shock

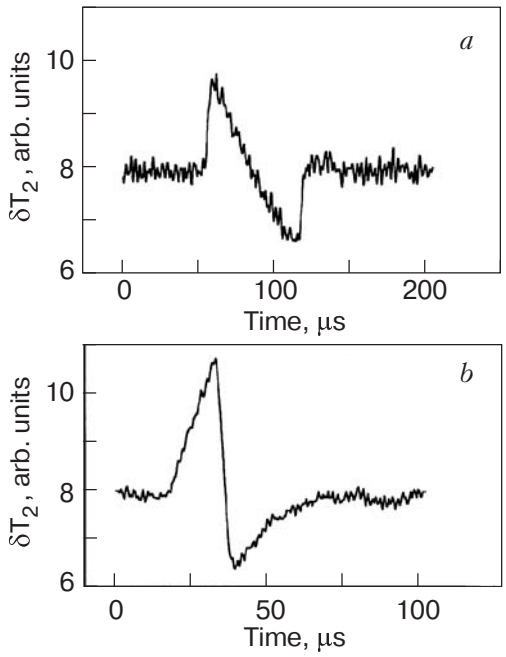

Fig. 3. Shape of a travelling three-dimensional second sound pulse generated by a point-like heater; $T = 1.50$ K ($\alpha > 0$) (*a*), $T = 2.02$ K ($\alpha < 0$) (*b*). The heater pulse duration was $\tau_e = 10$ μs.

wave of compression before the $\delta T_2(U)$ curves saturate. We may infer, first, that a significant part of the energy could be expended in the creation of this wave and, secondly, that vortices can be generated initially by the shock wave of first sound propagating ahead of the second sound shock wave.

It is known [6] that, if a three-dimensional (spherical) second sound wave is generated in He II by a point-like heater, then the propagating wave of heating (compression) is followed by a wave of cooling (rarefaction), see Fig. 3. In the range of temperatures $T_\alpha < T < T_\lambda$, where the nonlinearity coefficient is negative, the temperature discontinuity (the shock) is created at the centre of a running pulse. Consequently, the duration of the pulse does not change with the distance propagated [6,14] (see Fig. 3,*b*). This feature is important, e.g., for easier investigation of nonlinear and dissipative phenomena in the close vicinity of T_λ in He II, especially at elevated pressures.

2.2. Propagation of nonlinear second sound waves in compressed He II

Thermodynamic characteristics of He II such as the heat capacity C, the second sound velocity u_{20}, and the temperature of the phase transition T_λ, change considerably upon changing the pressure. The dependence of the nonlinearity coefficient on pressure (see above) was discussed in detail in the papers [12,18].

Figure 4,*a* shows the dependence of the nonlinearity coefficient α on temperature for $P = P_{SVP}$ (curve *1*) [2] and for elevated pressures [18] of $P = 5$, 10, 15, and 25 atm (curves *2*–*5*), respectively. The dependences $\alpha(P,T)$ for $P > P_{SVP}$ were calculated by using equation (1) and known dependences [3] for the heat capacity $C(P,T)$ and the second sound velocity $u_2(P,T)$. It can be seen from Fig. 4,*a* that the temperature T_α decreases from 1.8 to 1.58 K as the pressure is increased up to 25 atm.

The pressure dependence of T_α, the temperature at which the nonlinearity coefficient of second sound in He II passes through zero, is shown by the dotted curve in Fig. 4,*b*. The circles correspond to our experimental data. The dependence $\alpha(T)$ at fixed pressure was obtained from experimental observations of the evolution in shape of the planar shock second sound pulse with changing bath temperature T or heat flux density W. It is evident that the experimental data agree well with the results of our computations. The solid curves in Fig. 4,*b* were reconstructed from the data available in the literature [3]. They describe the temperature dependence of the solidification pressure and the pressure dependence of the superfluid transition temperature T_λ.

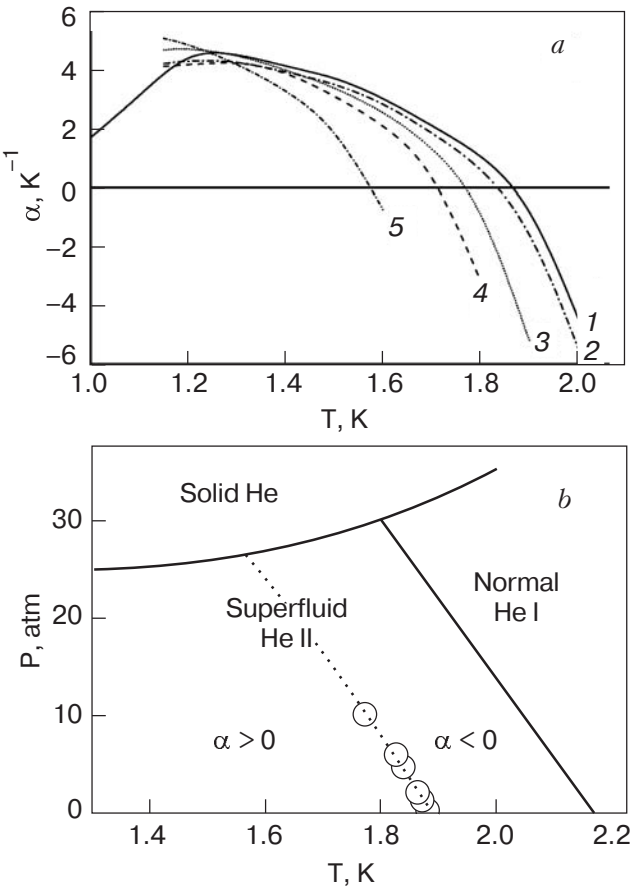

Fig. 4. Numerical evaluations of the dependence on pressure of the nonlinearity coefficient of second sound α, at SVP (curve *1*), and for different elevated pressures in the superfluid: P (atm) = 5 (*2*), 10 (*3*), 15 (*4*), and 25 (*5*) (*a*). Dependence on pressure of the temperature T_α at which α changes sign (*b*). On the plot (*b*) the dotted curve corresponds to theory; circles describe the experimental results; full lines show the temperature dependence of the pressure of solidification and the variation of the phase transition temperature T_λ with the pressure.

It follows from Fig. 4,*b* that, at all pressures up to that of solidification, there exists a fairly wide temperature range $T_\alpha < T < T_\lambda$ below T_λ, in which the nonlinearity coefficient of the second sound α is negative. According to Fig. 3,*b*, in this range the bipolar pulse of second sound propagating into the bulk of He II from a point-like heater should transform to a shock wave of constant duration with the discontinuity placed at its centre. These are important considerations for studies in the vicinity of T_λ at elevated pressures.

2.3. Nonlinear second sound in superfluid ^{3}He – ^{4}He *mixtures*

The nonlinearity coefficient of second sound in a dilute superfluid ^{3}He – ^{4}He solution is given by the following expression (see Refs. 19, 20 for details)

$$\alpha = \frac{3\rho_s A(\partial\sigma/\partial T)}{2\rho_n \bar{\sigma} u_{20}^2}, \qquad (4)$$

where

$$A = u_2^2\left(\frac{\rho_n}{\rho_s}\right)^2\left[2\frac{\rho_s}{\rho_n} + \frac{\bar{\sigma}}{(\partial\sigma/\partial T)}\frac{\partial}{\partial T}\left(\frac{\rho}{\rho_n}\right) + c\frac{\partial}{\partial c}\left(\frac{\rho}{\rho_n}\right)\right] -$$
$$- \frac{1}{3}\frac{\sigma^3}{(\partial\sigma/\partial T)^3}\left(\frac{\partial^2\sigma}{\partial T^2}\right) - \frac{\sigma^2 c}{\rho(\partial\sigma/\partial T)}\left(\frac{\partial\rho}{\partial c}\right) + \frac{1}{3}c^3\frac{\partial^2}{\partial c^2}\left(\frac{Z}{\rho}\right) -$$
$$- \frac{\sigma c^2}{(\partial\sigma/\partial T)}\left(\frac{\partial^2\sigma}{\partial c^2}\right) - \frac{\sigma^2 c}{(\partial\sigma/\partial T)}\frac{\partial}{\partial T}\left(\frac{\partial\sigma/\partial c}{\partial\sigma/\partial T}\right). \qquad (5)$$

We use here a conventional notation [2] such that: $c = x/\rho$ is the mass concentration of ^{3}He impurity; σ is the entropy per unit mass; $\bar{\sigma} = \sigma - c(\partial\sigma/\partial c)$; and Z is the thermodynamical potential for impurity particles.

Figure 5 illustrates the temperature dependence of the nonlinearity coefficient α in superfluid ^{4}He — ^{3}He mixture, calculated from Eqs. (4), (5) for molar ^{3}He content $x = 4.6$, 7, and 10%. Data from Ref. 21 were used in the calculations. The curve drawn for $x = 0$ (pure superfluid ^{4}He) corresponds to the curve *1* on Fig. 4,*a*. It can be seen from Fig. 5 that the temperature T_α at which the nonlinearity coefficient changes its sign is reduced from 1.88 K for pure superfluid ^{4}He to 1.67 K for superfluid mixture with $x = 10\%$ of ^{3}He impurity. Note here that the temperature T_λ of the superfluid transition is reduced from 2.17 K in pure superfluid ^{4}He to 2.02 K in mixture with ^{3}He content $x = 10\%$. This means that for dilute solutions there exist a rather wide interval of temperatures below T_λ for which $\alpha < 0$.

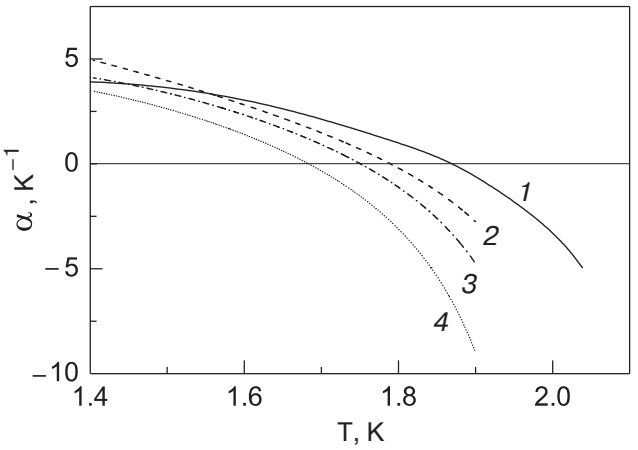

Fig. 5. Dependence on temperature of the nonlinearity coefficient of second sound α in superfluid ^{3}He — ^{4}He solutions under SVP at different ^{3}He concentrations x, %: 0 (*1*), 4.6 (*2*), 7 (*3*), and 10 (*4*).

2.4. Peculiarities of the generation of second and first sound waves by a film heater in He II *at high heat flux density*

We have studied the evolution in shape of the first sound wave that is excited, together with the second sound wave, by a heater in superfluid He II at elevated pressures.

We recall (see above) that, for all W, a pulsed heater in He II should excite ordinary first sound (pressure/density waves) as well as second sound (entropy/temperature waves). The thermal expansion coefficient β of He II is negative at temperatures above 1.2 K, $\beta = -(1/\rho)(\partial\rho/\partial T)_s < 0$ (here ρ is the density of bulk liquid). So, a quasi-adiabatic plane linear wave of first sound (the wave of heating of amplitude $\delta T_1 > 0$), excited by a heater, is a wave of rarefaction: $\delta\rho = \rho\beta\delta T_1 < 0$.

At low heat flux densities W, the energy contained in the first sound wave is much less than that in the second sound wave. For this reason, the amplitude δT_1 of the temperature oscillations in quasi-adiabatic first sound should be much smaller than the amplitude δT_2 of the second sound wave. Using the relations presented in Refs. 1, 2, 4 one can estimate that at small pressures close to SVP ($P \le 0.05$ atm), the amplitude ratio is very small $\delta T_1/\delta T_2 \approx 2\cdot 10^{-4}$. Therefore in experiments with linear second sound waves amplitude $\delta T_2 < 1$ mK, the amplitude of the first sound wave excited by a heater should be $\delta T_1 < 0.2$ μK. This value is beneath the typical resolution of a superconducting bolometer. But at high heat flux densities, at which the amplitude of the second sound wave was close to saturation (Fig. 2), the bolometer had registered arrival of the first sound wave of compression (a shock wave with $\delta\rho > 0$ and $\delta T < 0$). Creation of the shock wave of the first sound was associated typically with the film boiling of superfluid liquid at the surface of the heater at pressures below the critical pressure in He II (further discussion see below).

It follows from our computations based on the two-fluid model [2] that, in the linear approximation, the amplitude of the first sound wave should increase with increasing pressure in He II bath, for any given temperature T and given heat flux density W. Figure 6 demonstrates the dependence on temperature of the derivative $(\partial P/\partial T)_s$ in a quasi-adiabatic first sound wave in both He II and He I, calculated for different pressures P. A jump in the dependence at a given pressure arises due to the discontinuity in the temperature dependence of the thermal expansion coefficient β that occurs at a temperature slightly above T_λ (for example, in He I at $P = P_{SVP}$ the β coefficient changes both its value and sign from negative to positive at

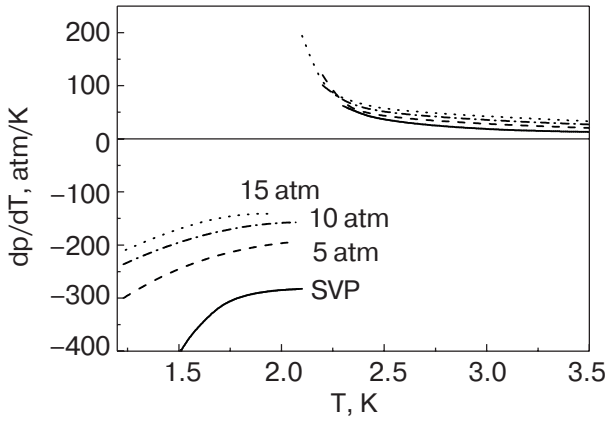

Fig. 6. Temperature dependence of the derivative $(\partial P/\partial T)_s$ in a quasi-adiabatical wave of first sound in liquid helium, calculated for the pressures P shown.

$T = T_\lambda + 0.006$ K [21]). Figure 7 shows the calculated ratio of amplitudes of temperature oscillations $\delta T_1/\delta T_2$ in linear waves of first and second sound emitted by a film heater in superfluid He II at different pressures P. It follows from Figs. 6, 7 that the temperature oscillations in the wave of first sound generated by a heater immersed in the superfluid should increase considerably with rising pressure P. It follows from Fig. 8 that, as the pressure is increased up to 15 atm, the ratio $\delta T_1/\delta T_2$ at $T = 1.9$ K increases by an order of magnitude.

Consistent with earlier work [4,22], we were unable to detect the linear waves of heating due to first sound in He II within the resolution of our bolometer (threshold about $5 \cdot 10^{-6}$ K) for pressures below 10 atm. The amplitude of a linear wave of the first sound could not be increased significantly by increasing the heat flux density W: at high W the bolometer detected the arrival of a wave of cooling of the first sound, i.e., a compression wave ($\delta T_1 < 0$, $\delta\rho > 0$) instead of a wave of heating.

On increasing the pressure to 13.3 atm, the bolometer detected the propagation in bulk He II of both waves of heating — *linear* first sound waves of rarefaction and second sound waves of compression, with heater pulses of relatively small W. With increase of W, first sound waves of rarefaction were transformed into waves of compression (cooling), and then into a shock sound wave with its discontinuity (a stepwise jump of pressure and temperature) situated at the front of the running wave.

The threshold for creation of a first sound compression wave was observed at pressures both below the critical pressure ($P_{cr} = 2.2$ atm) and above it where no liquid-vapor interface can exist. In the latter case, film boiling near the surface of the pulsed heater is obviously impossible. Creation of the wave of compression in He II can be attributed to the strong expansion of a normal He I layer created at the heater-fluid interface for $W > W_{cr}$: see discussion below. Note here, that in He I the thermal expansion coefficient β is positive, and its value is unusually high, about 10^{-2} K^{-1}. We observed a change in sign of the shock wave of compression when the temperature of the bath was increased above T_λ. As mentioned above, at pressures below the critical pressure one should also take account of pulse film boiling of helium at the interface.

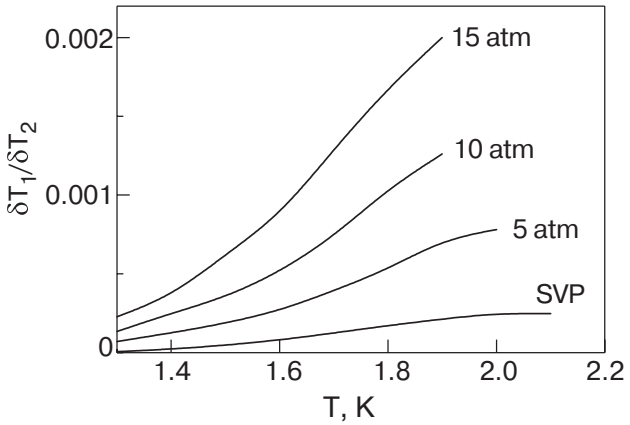

Fig. 7. Numerical computations of the ratio of the amplitudes of temperature oscillations $\delta T_1/\delta T_2$ of linear first and second sound generated by a plane heater in He II for the indicated pressures.

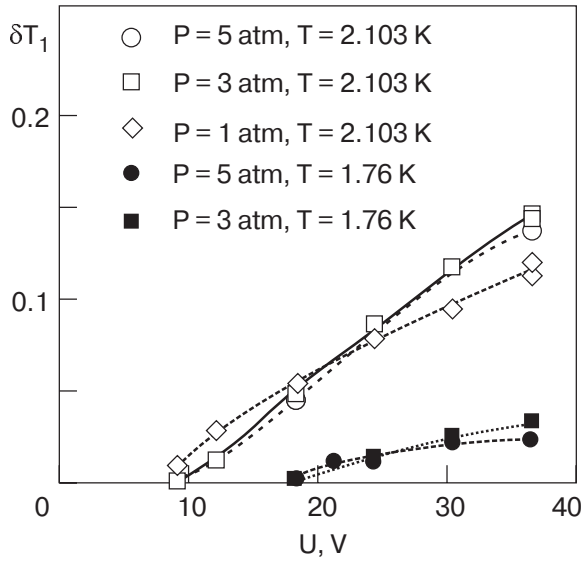

Fig. 8. Dependence of the amplitude δT_1 of the temperature oscillations in the shock first sound wave of compression ($\delta\rho > 0$, $\delta T_1 < 0$) on the voltage U, measured at pressures $P = 1$, 3, and 5 atm and temperatures $T = 2.1$ and 1.76 K. The heater pulse duration was $\tau_e = 10$ μs. The waves of compression were registered by the bolometer at high heat flux densities $W > 10$ W/cm^2.

Typical dependences of the amplitude of temperature oscillations in the first sound waves δT_1 (in arbitrary units) in He II at pressures $P = 1$, 3, and 5 atm and temperatures $T = 2.1$ K and 1.76 K on the voltage U of the heater pulse are shown in Fig. 8. The average heat flux density emitted by the heater in these experiments can be estimated from the relation $W = 0.1U^2$ W/cm^2. The heater pulse duration is constant at $\tau_e = 10$ μs. Open circles, squares, and diamonds correspond to $T = 2.10$ K and $P = 5$, 3, and 1 atm, respectively; solid circles and squares correspond to $T = 1.76$ K and $P = 5$ and 3 atm.

It should be emphasized that similar voltage dependences $\delta T_1(U)$ were observed at other pressures between 1 and 9 atm. In all cases the bolometer detected initiation of the first sound shock wave of cooling (compression) with $\delta T_1 < 0$, $\delta\rho > 0$, just as in previous studies [4,6]. As can be seen from Fig. 8, the cooling shock waves were created at heat flux densities beyond some critical value W_{cr}, which is equal to about 10 W/cm^2 for $T = 2.1$.K and about 30 W/cm^2 for $T = 1.76$ K. These values are of the order of the heat flux densities at which saturation of the second sound pulse amplitude takes place, as can be seen in Fig. 1.

Usually, saturation of the $\delta T_2(U)$ curve at high W is attributed to the interaction of the running second sound pulse with vortices [17]. It follows from our measurements that account should also be taken of the possible formation of vortices at the heater-fluid He interface; they can also be generated by the first sound shock wave propagating along a waveguide ahead of the shock wave of second sound.

Figure 9 shows the oscillograms illustrating the evolution of shape of the first sound pulses in compressed He II at $P = 13$ atm and $T = 1.895$ K with increasing heat flux density. The heater pulse duration τ was 3 μs. The numbers beside the curves indicate the voltage U applied to the heater. A detailed picture of the evolution of the shapes of first sound pulses of different initial duration, from 0.3 to 10 μs, has been presented earlier [23].

The curves plotted in Fig. 9 provide a clear illustration of the transformation of the wave of heating (rarefaction) into the wave of cooling (compression) with increasing heat flux density, for U above 15 V. It can be seen that the wave of compression is accompanied by a wave of heating (rarefaction), which is formed at the moment when the heater pulse is switched off. The wave of compression is associated with the pulsed thermal expansion of the layer of He I created at the heater-fluid He interface in the process of heating. Similarly, the subsequent wave of rarefaction might be attributed to a fast contraction of the liquid layer when the heat flux was switched off.

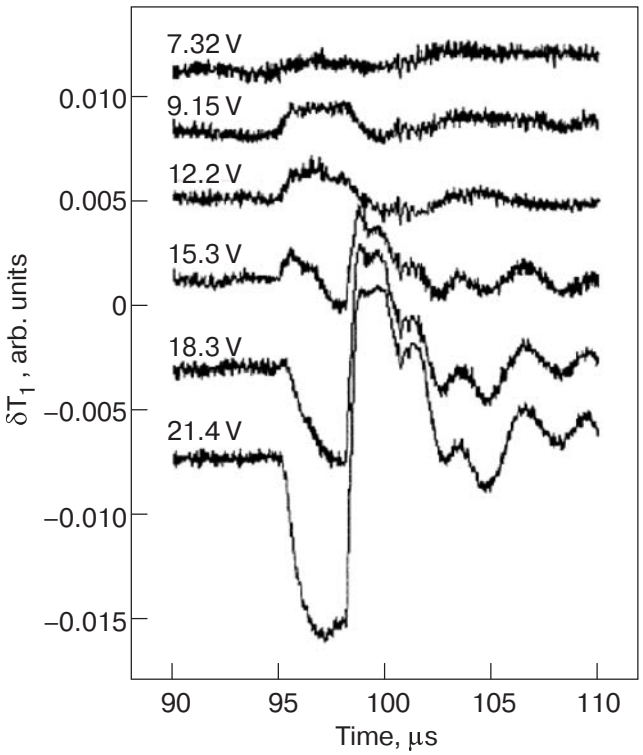

Fig. 9. Evolution of shape of the first sound wave in compressed He II for $P = 13$ atm, $T = 1.895$ K, heater pulse duration $\tau_e = 3$ μs. Numbers on the oscillograms indicate the voltage U at the heater.

The dependence of the first sound pulse amplitude δT_1 (in arbitrary units) on the voltage applied to the heater, for different τ is presented in Fig. 10. The heat pulse duration is marked on the plots. The solid points correspond to a rarefaction wave, and the open points correspond to a compression wave. As might be expected, the straight line $\delta T_1^{1/2} \sim U$ drawn through the solid points passes through the origin of coordinates.

We estimated the ratio of the slopes of the straight lines $\delta T_1^{1/2} = k_1 U$ and $\delta T_2^{1/2} = k_2 U$ describing for small U the dependences of the amplitudes $\delta T_1 = f(U)$ and $\delta T_2 = f(U)$ of linear first and second sound waves of heating excited in He II. The ratio of the coefficients calculated from the data shown in Fig. 7 is equal to

$$k_2 / k_1 = (\delta T_2 / \delta T_1)^{1/2} \approx 23. \qquad (6)$$

We also evaluated the ratio of the slopes of the straight lines drawn through the experimental points describing the dependence of the amplitudes δT_1 of the first sound waves and the amplitudes δT_2 of the second sound waves in He II at $P = 13.3$ atm and $T = 1.895$ K at given τ. The ratio of the slopes calculated for $\tau = 1$, 3, and 10 μs lies in the range $k_2/k_1 = 23 \pm 6$, which clearly agrees with the result (6) obtained in the linear approximation.

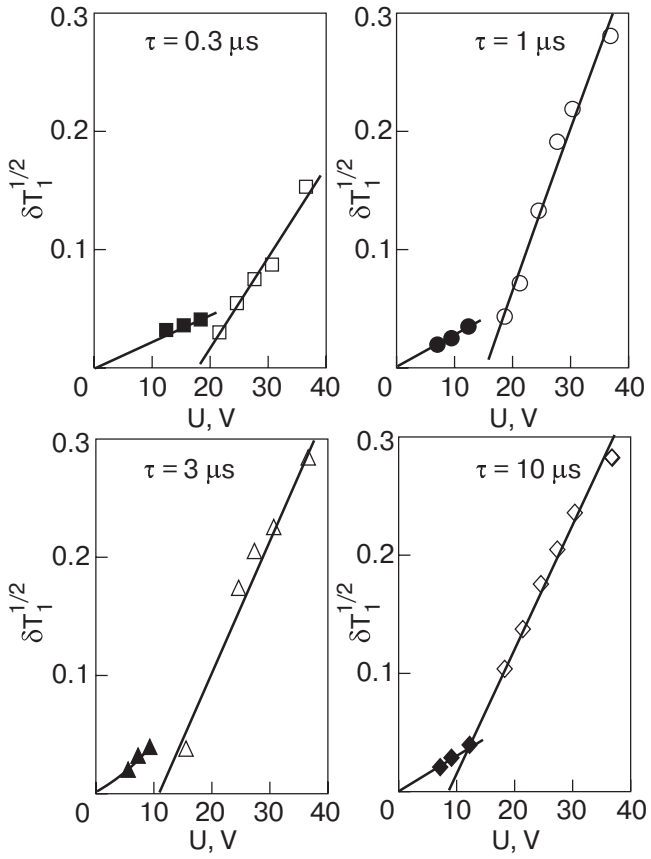

Fig. 10. Dependence of the amplitude δT_1 of the first sound pulse on the heater pulse voltage U, plotted as $\delta T_1^{1/2}$ vs. U. The pressure was $P = 13.3$ atm, the temperature was $T = 1.895$ K, and the heater pulse duration was $\tau_e = 0.3$, 1, 3, and 10 μs as indicated. The solid symbols correspond to the wave of rarefaction, and open symbols correspond to the wave of compression.

The threshold heat flux W_{cr}, above which a compression wave is observed, can be estimated from the abscissa intersections of the lines drawn through the open symbols in Fig. 10. It turned out that, for a given temperature, the product $W_{cr}\tau^{1/2}$ remains close to a constant as τ increased from 0.3 to 10 μs in the range of pressures of 1–13.3 atm (compare, e.g., Figs. 8 and 10), whereas the value of the product increases with reduction of the temperature below T_λ. The observed transformation from a wave of rarefaction to a wave of compression of first sound indicates that the heat transfer mechanism at the heater-He II interface changes qualitatively for a heat flux density above the critical level W_{cr}. As mentioned above, the appearance of the first sound waves of compression in superfluid He II at elevated pressures should be attributed to the strong thermal expansion of a layer of normal liquid He I created at the heater-He II interface at high heat loads. At low pressures $P << P_{cr}$, pulse film boiling was previously supposed to be the principal mechanism leading to the excitation of the first sound shock waves, and this additional effect must also be taken into account.

3. Nonlinear dynamics of standing second sound waves in a high-quality resonator filled with He II

In this Section we present the results of our recent studies of nonlinear second sound wave interactions in a high quality (high-Q) cylindrical resonator filled with He II.

The inner construction of the experimental cell was similar to that used in earlier investigations of planar second sound pulses [5,12]. The resonator was formed by a cylindrical quartz tube $L = 7$ cm in length and $D = 1.5$ cm in diameter, whose ends were capped by a pair of flat, parallel, quartz plates. Second sound waves were generated by a film heater on one plate and were detected by a superconducting film bolometer on the opposite plate. The resistance of the heater was $R = 35\ \Omega$ at $T = 2$ K. The sensitivity of the bolometer was varied from 1.2 to 2.6 V/K at temperatures $1.79\ \text{K} < T < 2.08$ K.

The frequency of the second sound wave $f_d = 2f_g$ excited by such a heater is twice the frequency f_g of the generator. This frequency doubling occurs because the heat flux from the heater is proportional to the *squared* voltage applied to the heater, $W(t) \propto U^2(t)$, where $U(t) = U_g \sin(2\pi f_g t)$ is the voltage applied to the heater. The signal from the bolometer was taken to a preamplifier, digitized with an analog-to-digital converter, and recorded on the hard disk of a computer. Before being recorded, each signal was averaged automatically over 6–8 measurements to reduce electrical noise.

Figure 11 shows the dependence of the amplitude of the recorded signal on the driving frequency f_d, at

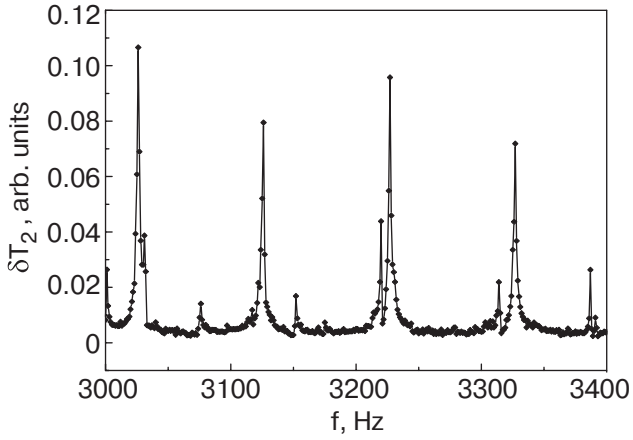

Fig. 11. Frequency dependence of the amplitude of a standing second sound wave δT_2 generated by the heater in the cylindrical resonator at $T = 2.075$ K. The driving voltage $U_g = 1.88$ V. The ac heat flux density $W = 0.02$ W/cm^2.

$T = 2.075$ K. The amplitude of the driving voltage was $U_g = 1.88$ V, so the ac heat flux density was W = $= 0.02$ W/cm^2. The peaks at the frequencies $f = 3020$, 3120, 3220, and 3320 Hz correspond to excitation of longitudinal standing second sound waves of frequencies

$$f_p = pu_2(T) \,/\, 2L \,,$$

where $p = 30$, 31, 32, and 33 are the resonance numbers. Other, smaller peaks correspond to the generation of radial modes in the cylindrical resonator. The Q-factor of the resonator determined from the data of Fig. 11 for longitudinal waves with $p > 10$ was $Q \sim 1000$.

We have observed a marked broadening of resonant peaks like those of Fig. 11 when the pulsed voltage applied to the heater exceeds $U_{g1} = 3.75$ V (i.e., at $W \geq 0.08$ W/cm^2). This phenomenon is believed to be attributable to interaction of the second sound wave with quantised vortex filaments, leading in turn to a nonlinear broadening of the resonances. In what follows below, we discuss *only* the results of measurements made at small $U_g < U_{g1}$.

Steady-state spectra of the standing second sound wave in a resonator were analysed by computing Fourier transforms of the signals. As an example, the spectrum of a signal recorded when driving at a frequency equal to the 11th longitudinal resonant frequency of the cell, $f_d = f_{11} = 1088$ Hz at $T = 2.075$ K, is shown in Fig. 12. It is clearly evident that the main spectral peak lies at the driving frequency f_d, and that high-frequency peaks appear at harmonics, $f_n = f_d \times n$, where $n = 2, 3\ldots$

It is seen that a cascade of waves is formed over a wide range of frequencies up to $f = 40$ kHz, i.e., up to

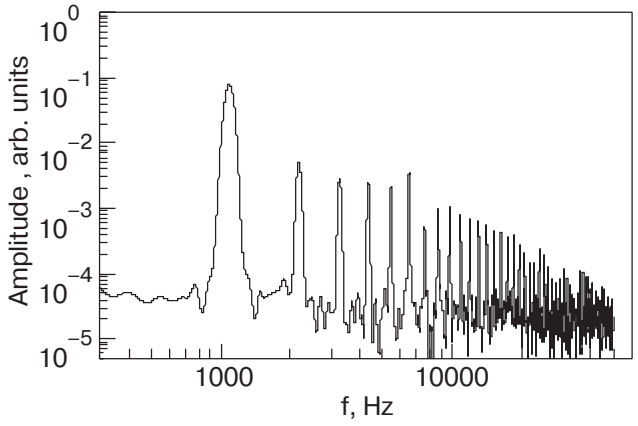

Fig. 12. Fourier spectrum of second sound waves computed from signals recorded when driving at the 11th longitudinal resonance frequency of the cell, $f_{11} = 1088$ Hz at $T = 2.075$ K. The driving amplitude was $U_g = 2.63$ V. The ac heat flux density $W = 0.06$ W/cm^2.

frequencies 40× higher than the frequency of the second sound f_{11} generated by the heater.

Following the general ideas formulated in papers [1,24,25] one can associate formation of the cascade with the establishment of a steady-state directed flux of the wave energy through the wavelength scales towards higher frequencies. Formation of this cascade is similar to the creation of the Kolmogorov distribution of fluid velocity over frequencies observed in classical liquids [1]. At high frequencies the amplitudes of harmonics are decreased. In this high-frequency domain the nonlinear mechanism for almost nondissipative transfer of the wave energy must change to viscous damping of the waves (cf. observations of high-frequency edge of the inertial range of frequencies in the system of nonlinear capillary waves on the surface of liquid hydrogen [26]), and the energy flux will then be absorbed due to viscous energy loss in this frequency domain. Observation of the cascade is in qualitative agreement with the results of our previous numerical studies [27,28] of nonlinear second sound standing waves in He II in a high-Q resonator. In papers [27,28] it was shown that, even if the amplitude of the periodic driving force is relatively small, a turbulent cascade of second sound waves of frequencies equal to multiples of the driving frequency should be formed over a wide range of frequencies when the Q-factor of the resonator is sufficiently high. Thus, we may infer that a wave turbulent state in the system of second sound waves has indeed been formed in the experiments in the frequency domain up to 40 kHz.

4. Conclusions

Our investigations have shown that, at all pressures up to that of solidification of He II, there exists a relatively wide temperature range below T_λ where the nonlinearity coefficient of second sound is negative. At these temperatures the shock front (the temperature discontinuity) is formed on the trailing edge of the plane wave, or at the center of a propagating bipolar second sound pulse of a finite amplitude generated by a point heater. The width of the bipolar pulse does not change with distance, so such pulses can be of a wide use in studies of nonlinear and dissipative phenomena in the vicinity of the superfluid transition line.

Observations of the transformation of the first sound waves of rarefaction to compression waves at heat flux density W higher than some critical value imply that the heat exchange mechanism at the pulsed heater-He II interface changes essentially above W_{cr}: the main reason for excitation of the compression waves in He II at pressures above the critical pressure is strong thermal expansion of the layer of normal

fluid He I arising at the interface for high W, accompanied by fast contraction of the layer after completion of the heat pulse. At pressures below P_{cr} one should consider also the film boiling of the liquid at the interface. Both the mechanisms explain the generation of the wave of compression (cooling) followed by a subsequent wave of rarefaction (heating) of the first sound in He II at high heat loads. All these processes should be taken into account in a discussion of the peculiarities of the behavior of first and second sound waves generated in superfluid helium by powerful heat pulses.

We have observed for the first time the creation of a cascade of standing second sound waves in He II in a high-Q resonator, formed at frequencies higher than that at which the system is driven, over a wide range of frequencies. The cascade is formed due to the nonlinear interactions between second sound standing waves in the resonator. At high frequencies the nonlinear mechanism of transfer of the wave energy is changed to viscous damping of the waves, thus terminating the cascade.

The authors are grateful to A.A. Levchenko, E.A. Kuznetsov, and V.V. Lebedev for valuable discussions. The investigations were supported by the Russian Foundation for Basic Research, project Nos. 05-02-17849 and 06-02-17253, by the Presidium of the Russian Academy of Sciences in frames of the programs «Quantum Macrophysics» and «Mathematical Methods in Nonlinear Dynamics», and by the Engineering and Physical Sciences Research Council (UK).

1. L.D. Landau and E.M. Lifshits, *Fluid Mechanics,* 2nd ed., Pergamon Press, Oxford (1987).
2. I.M. Khalatnikov, *An Introduction to the Theory of Superfluidity,* Benjamin, New York (1965).
3. S.J. Putterman, *Superfluid Hydrodynamics,* North-Holland Publishing Corp., Amsterdam (1974).
4. A.Yu. Iznankin and L.P. Mezhov-Deglin, *Sov. Phys. JETP* **57**, 801 (1983).
5. I.Yu. Borisenko, V.B. Efimov, and L.P. Mezhov-Deglin, *Fiz. Nizk. Temp.* **14**, 1123 (1988) [*Sov. J. Low Temp. Phys.* **14**, 619 (1988)].
6. L.P. Mezhov-Deglin, A.Yu. Iznankin, and V.P. Mineev, *JETP Lett.* **32,** 199 (1980).
7. L.S. Goldner, G. Ahlers, and R. Mehrotra, *Phys. Rev.* **43,** 12861 (1991).
8. S.K. Nemirovsky, *Usp. Fiz. Nauk* **160,** 51 (1990).
9. D.V. Osborne, *Proc. Phys. Soc. (London)* **A64**, 114 (1951).
10. A.J. Dessler and W.H. Fairbank, *Phys. Rev.* **104**, 6 (1956).
11. H.N.V. Temperley, *Proc. Phys. Soc.* **A64**, 105 (1951).
12. V.B. Efimov, G.V. Kolmakov, E.V. Lebedeva, L.P. Mezhov-Deglin, and A.B. Trusov, *J. Low Temp. Phys.* **119**, 309 (2000).
13. I.Yu. Borisenko, L.P. Mezhov-Deglin, and V.Zh. Rozenflantz, *Prib. Tekh. Exp.* No. 5, 137 (1987).
14. V.B. Efimov, G.V. Kolmakov, A.S. Kuliev, and L.P. Mezhov-Deglin, *Fiz. Nizk. Temp.* **24**, 116 (1998) [*Low Temp. Phys.* **24**, 81 (1998)].
15. L.S. Goldner, N. Mulders, and G. Ahlers, *J. Low Temp. Phys.* **93,** 131 (1993).
16. A. Ganshin and N. Mulders, *Phys. Rev.* **B69**, 172502 (2004).
17. L.P. Kondaurova, S.K. Nemirovskii, and M.V. Nedoboiko, *J. Low Temp. Phys.* **119,** 329 (2000).
18. V.B. Efimov, G.V. Kolmakov, L.P. Mezhov-Deglin, and A.B. Tusov, *Fiz. Nizk. Temp.* **25**, 551 (1999) [*Low Temp. Phys.* **25,** 407 (1999)].
19. G.V. Kolmakov, *Fiz. Nizk. Temp.* **29**, 667 (2003) [*Low. Temp. Phys.* **29**, 495 (2003)].
20. G. Kolmakov, L.P. Mezhov-Deglin, V.B. Efimov, and E.V. Lebedeva, *Phys. Status Solidi* **C1**, 3007 (2004).
21. B.N. Eselson, V.N. Grigoriev, V.G. Ivantsov, E.A. Rudavskii, D.G. Sanikidze, and I.A. Serbin, *Mixtures of Quantum Liquids* ^{3}He$-^4$He, *Nauka, Moscow* (1973) (in Russian).
22. M. Pomerantz, *Phys. Rev. Lett.* **26,** 362 (1971).
23. V.B. Efimov, G.V. Kolmakov, E.V. Lebedeva, L.P. Mezhov-Deglin, and A.B. Trusov, *JETP Lett.* **69,** 767 (1999).
24. A.N. Kolmogorov, *Doklady Akad. Nauk SSSR* **30**, 299 (1941).
25. V.E. Zakharov and R.Z. Sagdeev, *Doklady Akad. Nauk SSSR* **192,** 297 (1970).
26. G.V. Kolmakov, A.A. Levchenko, M.Yu. Brazhnikov, L.P. Mezhov-Deglin, A.N. Silchenko, and P.V.E. McClintock, *Phys. Rev. Lett.* **93**, 074501 (2004).
27. M.Yu. Brazhnikov, V.B. Efimov, G.V. Kolmakov, A.A. Levchenko, E.V. Lebedeva, and L.P. Mezhov-Deglin, *Fiz. Nizk. Temp.* **30**, 590 (2004) [*Low Temp. Phys.* **30**, 441 (2004)].
28. G.V. Kolmakov, A.A. Levchenko, M.Yu. Brazhnikov, V.B. Efimov, E.V. Lebedeva, and L.P. Mezhov-Deglin, *J. Low. Temp. Phys.* **138**, 525 (2005).